14

Principles of Total Neutron Counting

J. E. Stewart

14.1 INTRODUCTION

Total neutron counting accepts all pulses arising from neutron reactions (events) in the sensitive volume of a detector. No attempt is made to isolate events that occur nearly simultaneously as is done in coincidence counting.

A simple total neutron counting system consists of the components shown schematically in Figure 14.1. All detector events producing an amplifier output pulse with an amplitude greater than a threshold set by the integral discriminator are counted for a set time in a scaler. The usual choice of discriminator setting is high enough to reject low-amplitude pulses produced by gamma rays and electronic noise and low enough to count all neutron-induced pulses. It is important to note that the pulse-height spectra of ^{3}He and BF_3 neutron proportional counters contain no information about the energy of the detected neutrons. However, some information can be obtained through proper design of the moderating and absorbing materials surrounding the counters.

This chapter covers basic principles that are important in using total neutron counting for passive assay of materials containing uranium and plutonium. It does so using the example of polyethylene-moderated ^{3}He proportional counters. Such detectors are routinely used for a wide variety of neutron counting applications in nuclear facilities throughout the world.

14.1.1 Theory of Total Neutron Counting

The total neutron counting rate is given by the simple formula

$$T = \varepsilon M_L S \tag{14-1}$$

where T = total neutron count rate (counts/s)
ε = absolute detection efficiency (counts/n)
M_L = sample leakage multiplication (dimensionless)
S = sample neutron source intensity (n/s).

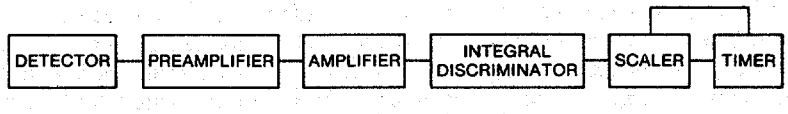

***Fig. 14.1** The basic components of a simple total neutron counting system.*

The absolute detection efficiency ε is the number of counts produced by the detector per neutron emitted from the sample. The sample leakage multiplication M_L is the number of neutrons emitted from the outer surface of the sample per neutron born inside the sample. The sample neutron source intensity S is the number of neutrons per second born in the sample.

The organization of this chapter is based on Equation 14-1. Factors affecting S, M_L, and ε are presented in relation to their influence on passive assays.

14.1.2 Comparison of Total and Coincidence Counting

Before describing the basic principles of total neutron counting, it is instructive to compare total neutron counting with coincident neutron counting. (Principles of neutron coincidence counting are described in detail in Chapter 16.) Generally, total neutron counting is responsive to *all* neutrons emitted from the sample, whereas coincidence counting responds only to the time-correlated neutrons.

The three important sources of neutrons for passive assays are (α,n) reactions, spontaneous fissions, and induced fissions (see Chapter 11 for a comprehensive description of neutron origins). The (α,n) reaction produces neutrons randomly in time. Fissions produce neutrons in bursts of 0 to 8. Coincidence circuitry can discriminate between neutrons produced from fissions and those produced in (α,n) reactions. This feature allows passive assay of plutonium nuclides with high spontaneous fission rates (most commonly ^{240}Pu) even in the presence of significant (α,n) reaction rates and room background. Also, active neutron coincidence methods use external sources of (α,n) neutrons to induce fissions in the sample, and the fission neutrons are counted using coincidence electronics. Total and coincident neutron counting are responsive in different ways to the three sources of neutrons in both passive and active assay, as shown in Table 14-1. Note that for active assay, the spontaneous fission neutron source can be made relatively small by choosing a strong (α, n) neutron source.

Table 14-1. Sensitivity of neutron counting techniques to the three sources of neutrons

Assay Method	Total Counting	Coincidence Counting
Passive Assay	(α,n), SF[a], IF[b]	SF, IF
Active Assay	(α,n), SF, IF	SF, IF

[a]SF - spontaneous fission neutrons.
[b]IF - induced fission neutrons.

Usually, the fewer neutron sources an assay technique is responsive to, the more specific it is to particular isotopes. The more isotope-specific the method is, the more useful it is for assay. In general, passive total neutron counting is the least isotope-specific of the techniques represented in Table 14-1. However, in those cases where only one of the three sources of neutrons dominates, passive total neutron counting can be used for assay. For example, UF_6 containing highly enriched uranium and PuF_4 are materials where the (α,n) source of neutrons dominates. Both uranium and plutonium

metal samples are examples where spontaneous fission is the dominant neutron source. In each of these examples, induced fission can be a complicating factor for both total and coincidence neutron counting. Because induced fissions increase the average multiplicity of simultaneous neutron emission from the sample and because the response of coincidence electronic circuits (for example, the shift register described in Chapter 16) increases faster than the average multiplicity, total counting is less sensitive to induced fission effects.

The coincidence count rate is proportional to ε^2 whereas the total count rate is proportional to ε. Variations in sample matrix materials (such as moisture) can alter the average energy of neutrons emitted from samples and thereby change the detector efficiency ε. Neutron coincidence counting is therefore more sensitive to changes in ε than is total counting. Also, total counting yields much better precision than coincidence counting in the same count time.

A disadvantage of total counting relative to coincidence counting is its sensitivity to background neutrons. Typically, background neutrons are randomly distributed in time and are easily discriminated by coincidence circuitry. A separate background count or neutron shielding or both are used to eliminate background total counts. In many cases, however, the background totals rate is insignificant compared to the totals rate from the sample and these measures are unnecessary.

In practice, total and coincidence neutron counting are often used together to correct sample/detector induced-fission (self-multiplication) effects. A complete discussion of this topic can be found in Chapter 16, Section 16.8.4.

14.2 PRIMARY NEUTRON PRODUCTION SOURCES

The first of the three important factors affecting total neutron counting is primary neutron production in the sample. Primary neutron production is from (α,n) reactions and spontaneous fission; secondary neutron production is from induced fission. Induced fission and neutron absorption in the sample are commonly considered together and called multiplication. Chapter 11 describes physical processes of primary neutron production and gives spontaneous fission and (α,n) reaction neutron yields from actinide isotopes of interest for passive neutron assays. Yields from (α,n) reactions are given for oxides and fluorides.

This section describes those features of neutron production in compounds of uranium and plutonium that affect assays based on total neutron counting. General calibration principles are discussed assuming no multiplication effects. In other words, neutron production by induced fission and neutron loss by neutron absorption are ignored. These topics are covered in Section 14.3, Neutron Transport in the Sample.

14.2.1 Plutonium Compounds

To apply total neutron counting as a signature for one or more isotopes of uranium or plutonium requires knowledge of the chemical form and isotopic composition of the sample. This point is well illustrated with examples. Consider 100-g samples of plutonium in the form of metal, PuO_2, and PuF_4 with three plutonium isotopic compositions representative of low-, medium-, and high-burnup fuel from light-water

reactors. Table 14-2 gives neutron production rates for each isotope, process, and form. The rates were computed from yields in Tables 11-1 and 11-3 in Chapter 11. Neutron production from spontaneous fission depends on the isotopic composition of the sample, but not on its chemical form. Neutron production from (α,n) reactions depends on both. The conclusions drawn from Table 14-2 are

(1) For plutonium metal, which has no (α,n) component, ^{240}Pu dominates primary neutron production (98, 96, and 65% for the three plutonium isotopic compositions).

Table 14-2. Primary neutron production rate in plutonium metal, PuO_2, and PuF_4 for three plutonium isotopic compositions

		Neutron Production Rate for 100 g of Pu (n/s)		
Isotope	Amount (wt%)	Metal (spontaneous fission)	PuO_2 (α,n)	PuF_4 (α,n)
^{238}Pu	0.024	62	322	52 800
^{239}Pu	89.667	2	3 416	502 135
^{240}Pu	9.645	9 838	1 360	202 545
^{241}Pu	0.556	0	1	95
^{242}Pu	0.109	187	0	29
^{241}Am	0.327[a]	0	880	144 417
	Totals	10 089	5 979	902 021
^{238}Pu	0.059	153	791	129 800
^{239}Pu	82.077	2	3 127	459 631
^{240}Pu	16.297	16 623	2 298	342 237
^{241}Pu	1.231	0	2	209
^{242}Pu	0.336	578	1	91
^{241}Am	0.162[a]	0	436	71 546
	Totals	17 356	6 655	1 003 514
^{238}Pu	1.574	4 077	21 092	3 462 800
^{239}Pu	57.342	1	2 185	321 115
^{240}Pu	24.980	25 480	3 522	524 580
^{241}Pu	10.560	0	14	1 795
^{242}Pu	5.545	9 537	11	1 497
^{241}Am	1.159[a]	1	3 118	511 863
	Totals	39 096	29 942	4 823 650

[a] ^{241}Am wt% relative to plutonium.

Total neutron counting of plutonium metal is a signature for the effective ^{240}Pu ($^{240}Pu_{eff}$) mass, where

$$^{240}Pu_{eff} = 2.43\,(^{238}Pu) + {}^{240}Pu + 1.69\,(^{242}Pu)\ . \tag{14-2}$$

The constants 2.43 and 1.69 account for the greater specific (per gram) spontaneous fission neutron production in ^{238}Pu and ^{242}Pu relative to ^{240}Pu. (Equation 14-2 differs slightly from Equation 16-1 (Chapter 16) for coincidence counting because of different neutron multiplicity distributions for the even plutonium isotopes.) If the plutonium isotopic composition is known, the total plutonium mass can be inferred from the $^{240}Pu_{eff}$ determination obtained from a calibration of the total neutron count rate. In other words (assuming a multiplication of 1),

$$T = \varepsilon\, S = k_0\, {}^{240}Pu_{eff} = k_1\, Pu \tag{14-3}$$

where k_0 and k_1 are empirical constants, and $^{240}Pu_{eff}$ and Pu represent $^{240}Pu_{eff}$ and plutonium masses, respectively.

(2) For PuO_2, the ratio of (α,n) to spontaneous fission neutron production is 0.59, 0.38, and 0.77 for the three plutonium isotopic compositions. Depending on composition, ^{238}Pu, ^{239}Pu, ^{240}Pu, and ^{241}Am are significant contributors to (α,n) neutron production in PuO_2. The total neutron production in PuO_2 is described by a generic equation of the form

$$S = a_1\,(^{238}Pu) + a_2\,(^{239}Pu) + a_3\,(^{240}Pu) + a_4\,(^{242}Pu) + a_5\,(^{241}Am) \tag{14-4}$$

where the multipliers a_1 through a_5 are specific neutron production rates for both spontaneous fission and (α,n) reactions in PuO_2 and the quantities in parentheses are plutonium isotopic masses. The multipliers are determined from plutonium isotopics and specific (α,n) and spontaneous fission yields for each isotope. If these are known, total plutonium mass can be determined from a calibration of the form

$$T = \varepsilon\, S = k_2\, Pu \tag{14-5}$$

where k_2 is an empirical constant and Pu stands for plutonium mass. Recall that Equation 14-5 assumes no multiplication effects ($M_L = 1$).

(3) For PuF_4, (α,n) reactions produce more than 98% of the neutrons for the three isotopic compositions. Generally, neutron production in PuF_4 is described by an equation similar to Equation 14-4,

$$S = a_6\,(^{238}Pu) + a_7\,(^{239}Pu) + a_8\,(^{240}Pu) + a_9\,(^{241}Am)\,. \tag{14-6}$$

The multipliers a_6 through a_9 are specific neutron production rates for (α,n) reactions in PuF_4 with small components from spontaneous fission. As with PuO_2, if plutonium isotopics are known, the total plutonium mass can be determined by total neutron counting of PuF_4 using the simple (multiplication-free) calibration

$$T = \varepsilon S = k_3 Pu . \quad (14\text{-}7)$$

Again, the constant k_3 must be determined empirically.

For the examples shown in Table 14-2, ^{241}Am values were taken at the time of analysis. Americium-241 is a daughter of ^{241}Pu. Americium-241 content increases with time because its half-life exceeds that of its parent. To calculate the ^{241}Am concentration at some time t knowing the initial concentrations of ^{241}Pu and ^{241}Am at time zero, use Equation 21-11 of Chapter 21.

14.2.2 Uranium Compounds

Just as for plutonium compounds, total neutron counting of uranium compounds requires prior knowledge of the chemical form and isotopic composition. Examples of uranium forms and compositions frequently found in the nuclear fuel cycle are characterized as to primary neutron production in Tables 14-3 and 14-4. Considered are 10-kg samples of uranium in the form of metal, UO_2, UO_2F_2, and UF_6. Table 14-3 treats ^{235}U enrichments of 0.2, 0.7, 3.0, and 18.2% (low-enriched uranium or LEU); Table 14-4 treats enrichments of 31.7, 57.4, 69.6, and 97.6% (high-enriched uranium or HEU). Spontaneous fission and (α,n) neutron rates are given by isotope and form for each enrichment. The rates were computed from yields in Tables 11-1 and 11-3 in Chapter 11 and from yields shown in Ref. 1 (UO_2F_2). The general conclusions drawn from these tables are

(1) Uranium-238 spontaneous fission dominates neutron production in uranium metal for ^{235}U enrichments below ~70%. This allows ^{238}U assay based on total neutron counting of large uranium metal samples for all but the highest ^{235}U enrichments. Because of the low neutron rates relative to plutonium metal, longer count time and larger samples are required for acceptable precision. Linear calibrations of total neutron count rate versus ^{238}U mass combined with ^{235}U enrichment are used for total uranium-metal determinations with low-enrichment material (see Chapter 15, Section 15.4.1, Box Counter). The calibration takes the form

$$T = \varepsilon S = k_4 {}^{238}U = k_5 U \quad (14\text{-}8)$$

where k_4 and k_5 are empirical constants.

(2) For UO_2, total neutron production [spontaneous fission plus (α,n)] is nearly constant for enrichments less than ~60%. With increasing enrichment, the spontaneous fission component decreases as the (α,n) component increases. At enrichments more than 60%, the (α,n) component grows rapidly. Uranium-234 alpha decay is the dominant source of (α,n) reactions in UO_2 for enrichments of 3% or greater. Total neutron production in UO_2 is generally described by

$$S = b_1 (^{234}U) + b_2 (^{235}U) + b_3 (^{238}U) \quad (14\text{-}9)$$

where b_1 through b_3 are specific neutron production rates for both spontaneous fission and (α,n) reactions in UO_2 and quantities in parentheses represent uranium isotopic masses. They are calculated from known isotopic compositions and specific neutron yields for each process. If these are known, a linear calibration of the form

Table 14-3. Primary neutron production rates in uranium metal, UO_2, UO_2F_2, and UF_6 for four uranium isotopic compositions (LEU)

		Neutron Production Rate for 10 kg of U (n/s)			
Isotope	Amount (wt%)	Metal (spontaneous fission)	UO_2 (α,n)	UO_2F_2 (α,n)	UF_6 (α,n)
^{234}U	0.0005	0	0	9	29
^{235}U	0.1977	0	0	1	2
^{236}U	0.0036	0	0	0	1
^{238}U	99.8	136	1	175	279
	Totals	136	1	185	311
^{234}U	0.0049	0	1	90	284
^{235}U	0.7108	0	0	3	6
^{236}U	-	-	-	-	-
^{238}U	99.28	135	1	174	278
	Totals	135	2	267	568
^{234}U	0.0244	0	7	449	1 415
^{235}U	3.001	0	0	11	24
^{236}U	0.0184	0	0	2	5
^{238}U	96.96	132	1	170	271
	Totals	132	8	632	1 715
^{234}U	0.0865	0	26	1 592	5 017
^{235}U	18.15	1	1	65	145
^{236}U	0.2313	0	1	28	67
^{238}U	96.96	111	1	143	228
	Totals	112	29	1 828	5 457

$$T = \varepsilon S = k_6 U \tag{14-10}$$

applies, where k_6 is an empirical constant and U stands for uranium mass. UO_2 as usually found in the nuclear fuel cycle (cans, rods, finished assemblies) suggests assay by active neutron techniques rather than passive, because the relatively low passive total neutron rates for standard sample sizes have to compete with room background. Active methods yield signals from ^{235}U-induced fission that are counted with coincidence electronics. Large UO_2 samples, however, may lend themselves to assay by passive total neutron counting depending on sample characteristics and measurement goals.

(3) For UO_2F_2 (a chemical reaction product of UF_6 and water), neutron production is dominated by the (α,n) component. Neutron production rates increase uniformly with ^{235}U enrichment. This is because ^{234}U is enriched along with ^{235}U in enrichment processes based on isotopic mass differences. Equations analogous to Equations 14-9

Table 14-4. Primary neutron rates in uranium metal, UO_2, UO_2F_2, and UF_6 for four uranium isotopic compositions (HEU)

		Neutron Production Rate for 10 kg of U (n/s)			
Isotope	Amount (wt%)	Metal (spontaneous fission)	UO_2 (α,n)	UO_2F_2 (α,n)	UF_6 (α,n)
^{234}U	0.1404	0	42	2 583	8 143
^{235}U	31.71	1	2	114	254
^{236}U	0.3506	0	1	42	102
^{238}U	67.80	92	1	119	190
	Totals	93	46	2 858	8 689
^{234}U	0.2632	0	79	4 843	15 265
^{235}U	57.38	2	4	207	459
^{236}U	0.5010	0	1	60	145
^{238}U	41.86	57	0	73	117
	Totals	59	84	5 184	15 986
^{234}U	0.3338	0	100	6 142	19 360
^{235}U	69.58	2	5	250	557
^{236}U	0.5358	0	1	64	155
^{238}U	29.55	40	0	52	83
	Totals	42	106	6 508	20 155
^{234}U	1.032	1	310	18 989	59 856
^{235}U	97.65	3	7	352	781
^{236}U	0.2523	0	1	30	73
^{238}U	1.07	1	0	2	3
	Totals	5	318	19 373	60 713

and 14-10 describe the passive total-neutron-counting calibration of UO_2F_2 with known isotopic composition. Passive total neutron counting has been used to quantify UO_2F_2 deposits inside process equipment in gaseous diffusion enrichment plants (Ref. 2).

(4) For UF_6 (the standard process material for uranium enrichment), ^{234}U alpha decay and the subsequent $^{19}F(\alpha,n)^{22}Na$ reaction dominate neutron production. The material is similar to UO_2F_2 with the (α,n) component being more dominant because of additional fluorine. For arbitrary enrichment, total UF_6 neutron production is also given by an equation analogous to 14-9. A calibration is then possible with an equation of the form of Equation 14-10.

Passive total neutron counting can be used for verification of UF_6 cylinders of all sizes. It is routinely used for cylinders containing low-enriched UF_6. It is fast, simple, and inexpensive. Small cylinders are counted in nearly 4π geometry ("well" counters). Large cylinders are counted with portable counters such as the "SNAP" (Chapter 15,

Section 15.2). For large, low-enrichment cylinders, simpler calibration expressions than those shown in Equations 14-9 and 14-10 are obtained by assuming a constant ^{238}U weight fraction and a constant ratio of ^{235}U to ^{234}U (see Chapter 15, Section 15.2.2). The data of Tables 14-2, 14-3, and 14-4 are plotted in Figure 14.2. Compared are total spontaneous fission plus (α,n) neutron production rates for plutonium, PuO_2, PuF_4, uranium, UO_2, UO_2F_2, and UF_6. The specific (per gram uranium or plutonium) rates span eight orders of magnitude from uranium metal to PuF_4. Rates are plotted as a function of wt% ^{235}U and ^{239}Pu. The plot is useful for visual comparison and for estimating counting statistics with known detectors and geometries.

14.2.3 Impurities

Rarely are the plutonium and uranium compounds found in the nuclear fuel cycle completely free of impurities. These impurities can significantly alter primary neutron

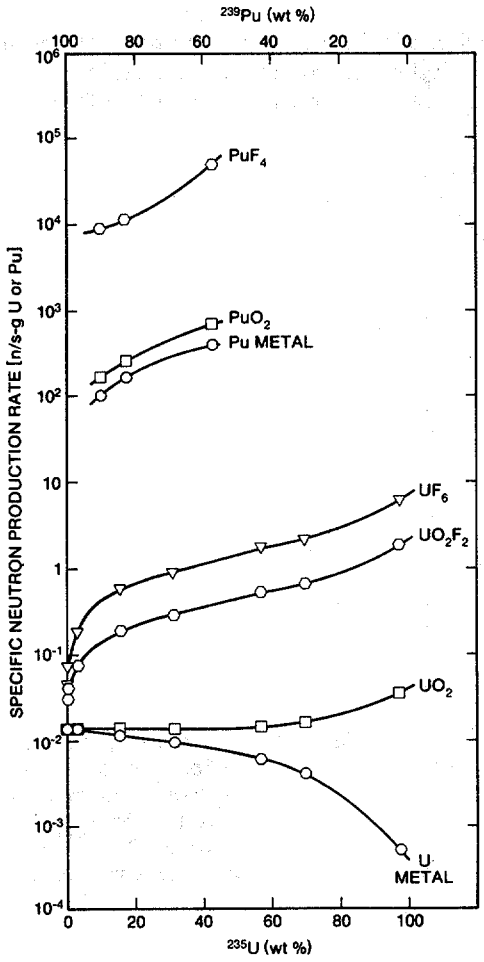

Fig. 14.2 Specific neutron production rates for uranium and plutonium metals, oxides, and fluorides. Data are from Tables 14-2 through 14-4.

production. As an example, consider PuO_2 with H_2O added. Water is commonly found in PuO_2 with a nominal value of 1 wt%. Table 14-2 gives dry PuO_2 (α,n) neutron production values for three plutonium isotopic compositions characteristic of low-, medium-, and high-burnup light-water reactor fuel. The first is approximately 10% ^{240}Pu by weight. The second is approximately 16% ^{240}Pu, and the third is approximately 25% ^{240}Pu. Figure 14.3 shows the dependence of (α,n) neutron production [S(α,n)] on weight percentage water for the three plutonium isotopic compositions. The quantity S(α,n) for the 25% ^{240}Pu material is roughly a factor of 5 higher than for the 16% and 10% materials (because of the high ^{238}Pu fraction) regardless of moisture content. Figure 14.4 displays S(α,n) values for wet relative to dry PuO_2 versus wt% H_2O. It is useful to note that the moisture effect is independent of plutonium isotopic composition. That is, adding 1 wt% moisture yields the same relative change in S(α,n) for 10%, 16%, and 25% ^{240}Pu, namely + 4.4%. This indicates that small changes in initial alpha-particle energies resulting from changes in plutonium isotopics do not significantly affect neutron production in wet PuO_2.

Although many trace contaminants are found in PuO_2, fluorine is usually the most significant for altering S(α,n). Figure 14.5 displays S(α,n) versus F contamination ir PuO_2 (16% ^{240}Pu) with 1 and 9 wt% H_2O. Figure 14.6 shows the S(α,n) values for PuO_2

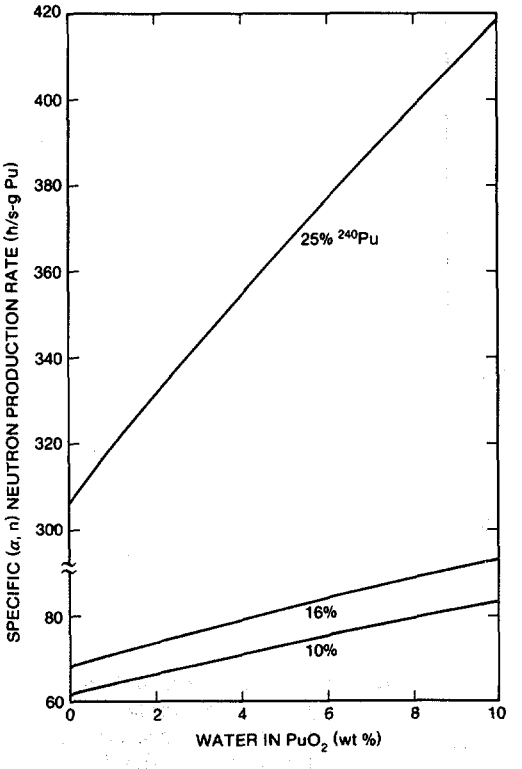

Fig. 14.3 *Specific neutron production rates from (α,n) reactions in PuO_2 versus added moisture for ~10% ^{240}Pu, ~16% ^{240}Pu, and ~25% ^{240}Pu plutonium isotopic compositions.*

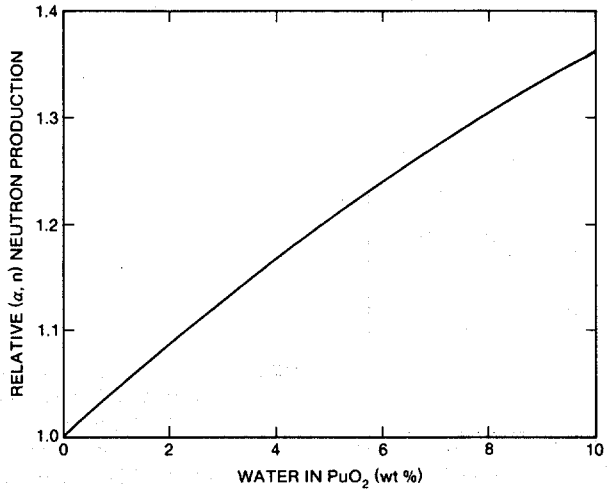

Fig. 14.4 *Neutron production from (α,n) reactions in wet relative to dry PuO_2 versus added moisture. The 10, 16, and 25% ^{240}Pu isotopic compositions fall on a single curve.*

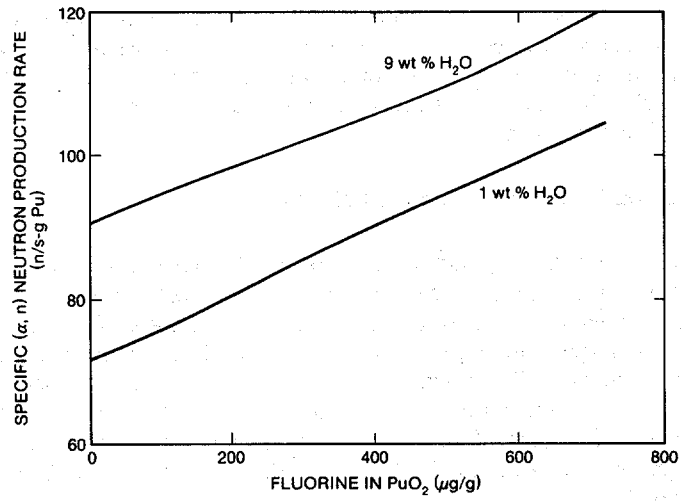

Fig. 14.5 *Specific neutron production rates from (α,n) reactions in PuO_2 versus fluorine contamination for 16% ^{240}Pu plutonium isotopic composition. Both 1 and 9 wt% H_2O cases are shown.*

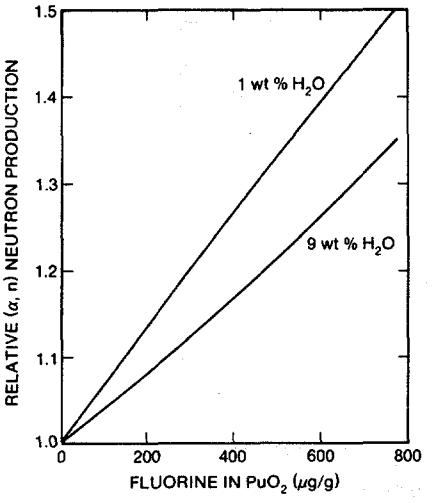

Fig. 14.6 *Neutron production from (α,n) reactions in PuO_2 with fluorine impurities relative to pure PuO_2 versus fluorine concentration for 16% ^{240}Pu. Both 1 and 9 wt% H_2O cases are shown.*

(16% ^{240}Pu) with fluorine impurities relative to pure PuO_2 versus fluorine concentration. Cases are shown for both 1 and 9 wt% moisture. The *relative* change in S(α,n) from F contamination is greater for dry than for wet PuO_2.

The H_2O and F impurities affect (α,n) neutron production but not spontaneous fission neutron production. If H_2O and F concentrations are known, data such as shown in Figures 14.3 through 14.6 can be used to adjust calibration parameters for total neutron counting assays. These data were calculated using the Los Alamos SOURCES code (Refs. 3, 4). Reference 5 contains results of calculations of the effects of several low-Z trace contaminants on S(α,n) for plutonium metal. Section 11.4 in Chapter 11 gives approximate formulas for calculating contributions to S(α,n) from impurities in uranium and plutonium oxides.

14.2.4 Neutron Energy Spectrum Effects

Neutrons are produced in spontaneous fission and (α,n) reactions with characteristic energy distributions or spectra. These are important in the design of total neutron counters using polyethylene-moderated ^3He detectors. For plutonium compounds, the spontaneous fission spectrum depends slightly on plutonium isotopic composition and not on sample chemistry. The spectrum is dictated by the nuclear kinematics of the spontaneous fission disintegration process, which differ slightly for ^{238}Pu, ^{240}Pu, and ^{242}Pu. Figure 14.7 is a plot of the specific spontaneous fission neutron production spectrum for plutonium with 16% ^{240}Pu. The ^{240}Pu spectrum is described well by the Watt form (Ref. 3)

$$N(E) \propto e^{-E/A} \sinh\left(\sqrt{BE}\right) \tag{14-11}$$

where E = laboratory neutron energy, A = 0.795, and B = 4.69.

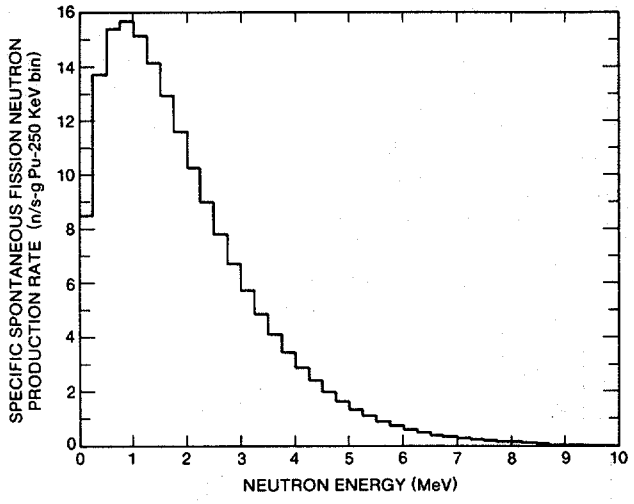

Fig. 14.7 *Specific spontaneous fission neutron production spectrum for Pu with 16% ^{240}Pu.*

The laboratory spectrum of neutron energies from (α,n) reactions in plutonium compounds depends on sample chemistry, impurity levels, and slightly on plutonium isotopic composition. Sample composition determines the slowing down spectrum of alpha-particle energies and the (α,n) reaction cross-section dependence on alpha-particle energy. Figure 14.8 displays four specific (α,n) neutron production spectra for PuO_2 (16% ^{240}Pu) with variable moisture and fluorine contamination. An increase in moisture "hardens" the spectrum slightly and an increase in fluorine "softens" it. Figure 14.9 shows the four total spectra corresponding to the moisture and fluorine concentrations of Figure 14.8. The average energies of these four spectra are not substantially different. This similarity indicates that spectral shape differences are generally not major factors affecting total neutron counting of PuO_2 with moisture and fluorine contamination levels in the ranges used. These ranges are typical of a wide variety of PuO_2 samples.

Figure 14.10 displays normalized neutron production spectra from (α,n) reactions in $^{234}UF_6$. Spectra for two ^{22}Na level branching schemes are shown. The $^{234}UF_6$ (α,n) spectrum is softer than that for PuO_2 with an average neutron energy of approximately 1.2 MeV. For PuO_2, the average is approximately 2.0 MeV.

14.2.5 Thin-Target Effects

In the previous sections, primary neutron production by (α,n) reactions was assumed to take place in samples that qualify as "thick targets." Thick targets are materials where alpha particles lose all their energy in the sample. If the sample density is low enough, neutron production is reduced because alpha particles escape before they undergo (α,n) reactions with target isotopes. Neutron production by ^{234}U alpha particles driving the

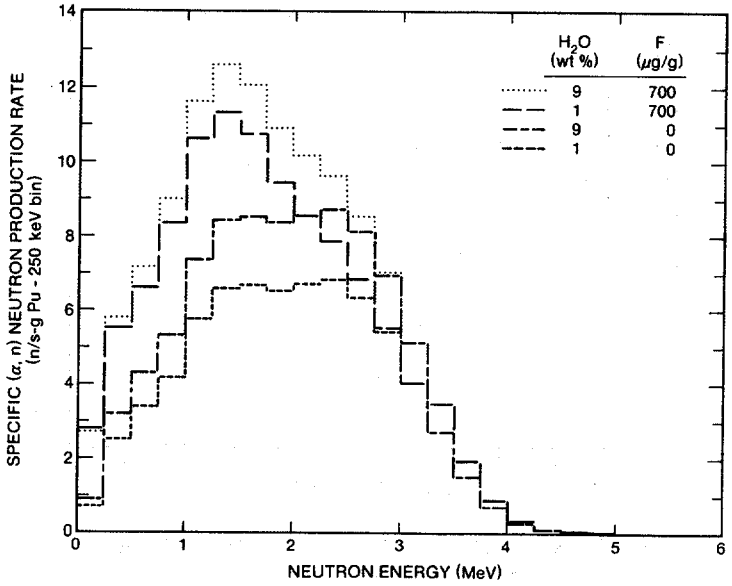

Fig. 14.8 Specific (α,n) neutron production rate spectra of PuO_2 (16% ^{240}Pu) with variable moisture and fluorine content (from SOURCES calculation [Ref. 3]).

$^{19}F(\alpha,n)^{22}Na$ reaction in gaseous UF_6 is a "thin-target" situation. In this case, alpha particles may escape the gas volume at energies above the $^{19}F(\alpha,n)$ cross-section threshold. Reference 6 presents methods for calculating thin-target neutron production in UF_6 gas. Figure 14.11 (from Ref. 6) displays UF_6 neutron production versus projected range. The projected range is the product of atom density and target thickness. Neutron production saturates above approximately 6×10^{19} atoms/cm^2 at the thick-target neutron production value for $^{234}UF_6$. At approximately 1.3×10^{19} atoms/cm^2, the number of neutrons produced per alpha particle is half the thick-target value.

14.3 NEUTRON TRANSPORT IN THE SAMPLE

After specifying the primary neutron production in the sample and relating that to grams of uranium or plutonium, the next logical step in using passive total neutron counting for assay is to consider the number of neutrons that escape the sample per neutron produced. Description of the transport of neutrons in the sample volume (including all the processes of neutron creation and loss) is complex and requires the use of Monte Carlo simulations on large computers for best results. Chapter 12 describes many of the basic principles of neutron transport. Here, we present a simple formula for sample leakage multiplication, discuss numerical results, and describe the use of the formula.

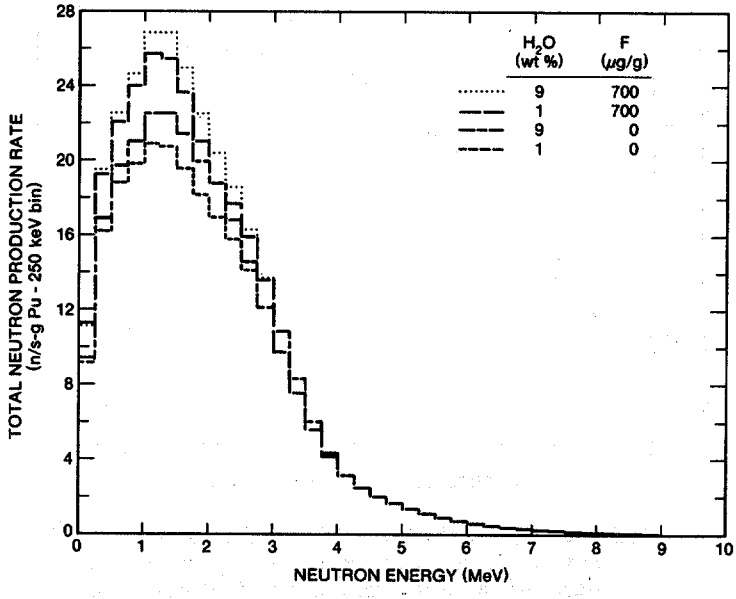

Fig. 14.9 *Total neutron production rate spectra of PuO_2 (16% ^{240}Pu) with variable moisture and fluorine content (from SOURCES calculation [Ref. 3]).*

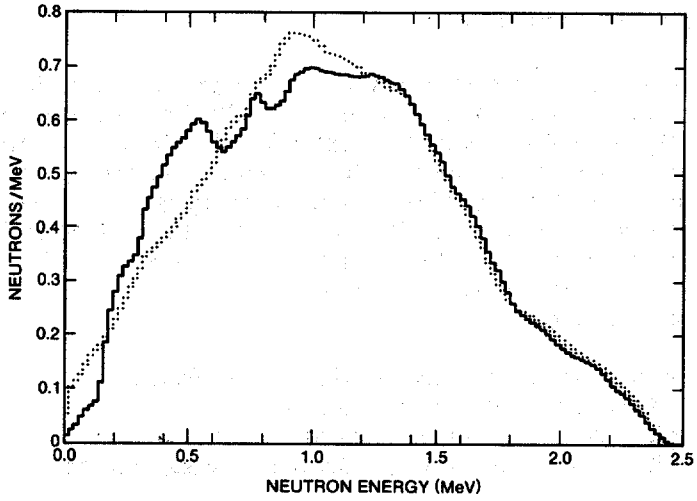

Fig. 14.10 *Normalized (α,n) neutron production spectra of $^{234}UF_6$ (from SOURCES [Ref. 3] calculation) with two ^{22}Na level branching models.*

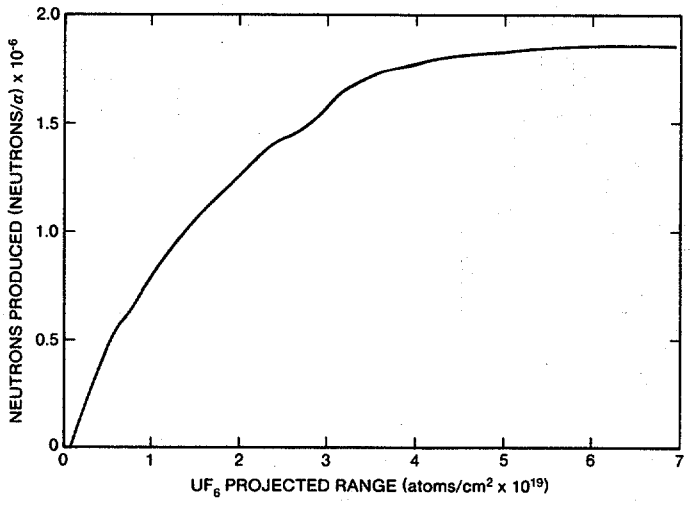

Fig. 14.11 *Neutron production by a 4.77-MeV alpha particle from ^{234}U decay versus projected range in UF_6. The range in cm can be obtained by dividing the abscissa by the UF_6 atom density (atoms/cm^3).*

14.3.1 Leakage Multiplication

The number of neutrons escaping the sample (and therefore available for counting) per primary neutron produced is called the leakage multiplication of the sample, M_L. The quantity M_L differs from the total multiplication M defined in Chapter 12. The quantity M is the number of neutrons *created* in the sample [from primary source events, induced fissions, (n,2n) reactions, and other events] per primary neutron produced. The quantity M_L accounts for neutron *creation and loss* in the fission and parasitic capture reactions. Therefore, M_L is more pertinent to total neutron counting than is M. The two quantities are closely related, as described below.

The following definitions apply:

ν = the average number of neutrons created by induced fission
p = probability that a neutron will induce a fission
p_c = probability that a neutron will be captured
p_L = probability that a neutron will escape the sample (leakage probability).

A neutron of a given generation can induce a fission with probability p and disappear with probability $1 - p$. In other words,

$$p + p_c + p_L = 1 \quad . \tag{14-12}$$

Also, the number of fissions produced in a given generation per fission in the previous generation is pν. The quantity pν is the multiplication factor k from reactor physics discussed in Chapter 12. In an induced fission a neutron is absorbed. Therefore the net neutron *profit* per fission is $\nu - 1$.

Consider a sample in which induced fission, neutron capture, and escape are the only possible fates of neutrons. In generation zero, one neutron is produced from spontaneous fission or an (α,n) reaction. In the first generation, there are p fissions and pν new neutrons created with a net neutron profit of $p(\nu - 1)$. In the second generation, there are $p^2\nu$ fissions, $(p\nu)^2$ new neutrons, and a net profit of $p^2\nu(\nu - 1)$. This multiplication process is shown in Table 14-5 for the first few neutron generations. For all generations, the sum of the number of neutrons created from a single source neutron is the total multiplication M.

$$M = \frac{1}{1 - p\nu} = \frac{1}{1 - k} \; ; \; k < 1 \quad . \tag{14-13}$$

For all generations, the sum of the net neutron profit is the total net neutron profit per source neutron $(1 - p)/(1 - p\nu)$. Not all the net neutron profit will escape the sample—some will be captured. The leakage multiplication M_L is the total net neutron profit per source neutron times the probability of escape divided by the probability of disappearance, that is,

$$M_L = \left(\frac{1-p}{1-p\nu}\right)\left(\frac{p_L}{p_L + p_c}\right) = \frac{p_L}{1-p\nu} = \frac{1-p-p_c}{1-p\nu} \quad . \tag{14-14}$$

Finally, from Equations 14-13 and 14-14, the relationship between M_L and M is

$$M_L = p_L M \quad . \tag{14-15}$$

If the probability of capture p_c is small,

$$M_L \simeq (1 - p)\, M = \frac{1 - p}{1 - p\nu} \quad . \tag{14-16}$$

Table 14-5. The neutron multiplication process through the fourth fission generation

Generation	Number of Fissions	Neutrons Created	Net Neutron Profit
0	—	1 (Source)	1
1	p	pν	$p(\nu - 1)$
2	$p(p\nu)$	$(p\nu)^2$	$p(p\nu)(\nu - 1)$
3	$p(p\nu)^2$	$(p\nu)^3$	$p(p\nu)^2(\nu - 1)$
4	$p(p\nu)^3$	$(p\nu)^4$	$p(p\nu)^3(\nu - 1)$

If both p_c and p are small, M_L and M are approximately the same. The quantity M is always greater than or equal to M_L.

Equation 14-14, the expression for M_L, depends on three parameters: ν, p, and p_c. These quantities depend on the energy of the neutron inducing a fission or being captured. Therefore, they are understood to represent averages over the slowing-down spectrum of neutron energies in the sample. All three parameters depend on sample composition and density. The probabilities p and p_c depend on sample geometry as well. Multiplication effects caused by neutrons reflecting off the counter back into the sample are understood to be included in p and p_c. Reflection lowers the neutron's energy and increases both p and p_c.

Figure 14.12 shows plots of the leakage multiplication M_L versus the fission probability p; Equation 14.16 was used to generate the plots. Two sets of curves are shown. The lower set of three curves is representative of uranium-bearing samples with $\nu = 2.5$. The upper set of three curves with $\nu = 3.0$ is representative of plutonium-bearing samples. In each set of curves, the capture probability p_c is varied from 0 to 0.02, which covers a wide range of samples.

Figure 14.13 shows plots of both total and leakage multiplication versus PuO_2 mass in a cylindrical volume with a diameter of 8.35 cm. The ^{240}Pu (effective) is 10 wt% of plutonium. The PuO_2 has a density of 1.3 g/cm^3 and contains 1 wt% H_2O. The sample fill height increases as PuO_2 mass increases. The leakage multiplication values were

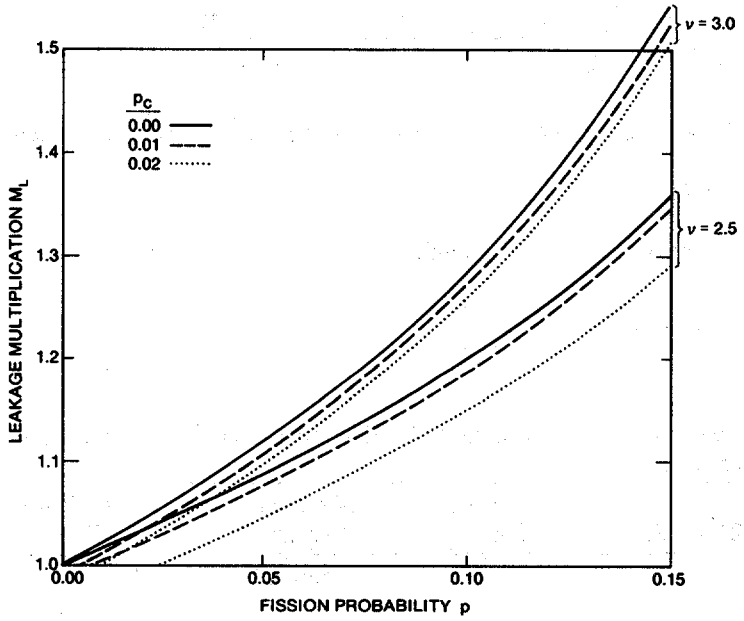

Fig. 14.12 *Leakage multiplication M_L versus fission probability for two values of the average fission neutron multiplicity and three values of the capture probability.*

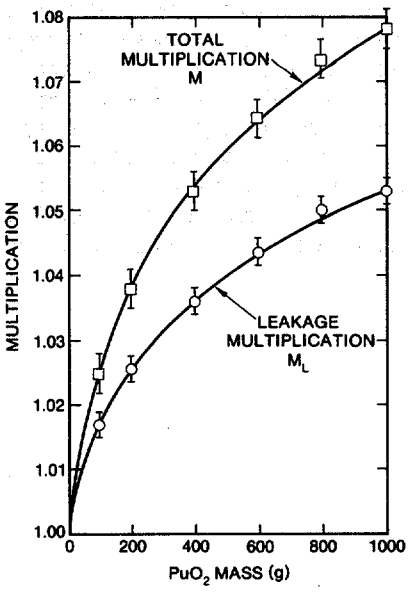

Fig. 14.13 *Leakage multiplication M_L and total multiplication M versus PuO_2 mass in a container with an 8.35-cm inside diameter. The plutonium is 10 wt% ^{240}Pu (effective). The sample PuO_2 has a density of 1.3 g/cm^3 and is 1 wt% H_2O. The fill height increases as mass is added.*

calculated using the Monte Carlo transport code MCNP (Ref. 7). The total multiplication values M were calculated from the leakage multiplication values M_L using the relationship

$$M = \frac{\nu M_L - 1}{\nu - 1} \tag{14-17}$$

with $\nu = 3.13$. This expression can be obtained by combining Equations 14.13 and 14.16. For the samples described by Figure 14.13, the capture probability p_c is negligibly small. The plots clearly show the difference in total multiplication M and leakage multiplication M_L. Reference 8 contains additional information on the MCNP calculations of M_L and information on coincidence multiplication corrections.

14.3.2 Leakage Spectra

Neutrons escaping from a sample have a lower average energy than when first produced in spontaneous fission or (α,n) reactions. Neutrons lose energy in the sample through elastic collisions with light nuclei and inelastic collisions with heavy nuclei. The sample container can also affect the neutron leakage spectrum, but is generally not a major factor. Unless there are intervening materials, the energy spectrum of neutrons escaping the sample container is the spectrum seen by the neutron detector. The shape of this spectrum can be important in determining detection efficiency, as described in Section 14.4.

An example of neutron energy losses in the sample, as calculated with the Monte Carlo Code MCN (Ref. 9), is shown in Figure 14.14. This figure shows the leakage spectrum of neutrons from a 5000-lb (2273-kg) cylinder of UF_6 whose ^{235}U enrichment is 2.5% (Ref. 10). For these calculations, a uniform spatial distribution of 1-MeV neutrons was assumed because the $^{19}F(\alpha,n)^{22}Na$ thick-target energy spectrum (Figure 14.10) was not well known at that time. Figure 14.14 shows the neutron moderation in the large UF_6 sample cylinder to be quite significant. The average energy of the leakage neutrons is 0.44 MeV compared with the average source neutron energy of 1.0 MeV. It should also be noted that about 20% of the source neutrons do not escape from the cylinder because of parasitic capture.

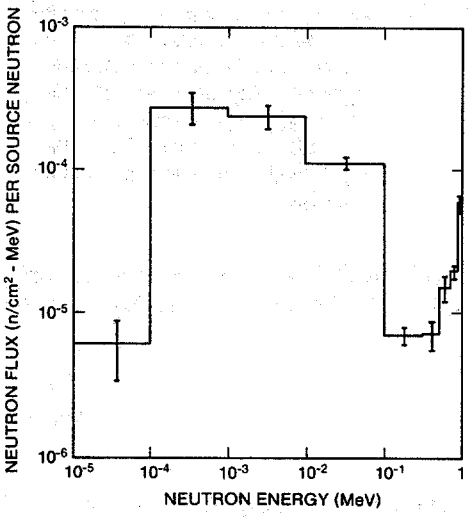

Fig. 14.14 *Neutron leakage spectrum from a 5000-lb UF_6 cylinder (2.5% ^{235}U) assuming uniformly distributed 1-MeV source neutrons.*

Another leakage spectrum calculation, performed with the MCNP Code (Ref. 7), is shown in Figure 14.15. The sample modeled is 800 g of PuO_2 with a density of 1.3 g oxide/cm^3. The sample contains 706 g of plutonium (10% ^{240}Pu) and 1 wt% water. The cylindrical sample is 8.35 cm in diameter and 11.24 cm in height. The smooth curve in Figure 14.15 is the ^{240}Pu spontaneous fission neutron emission spectrum (Figure 14.7 and Equation 14.11). The calculated sample neutron leakage spectrum is the histogram distribution, with 1σ error bars shown. The average energy of the leakage spectrum is 1.91 MeV compared with 1.93 MeV for the emission spectrum. This implies very little moderation of the source spectrum by this PuO_2 sample. The small buildup in the leakage spectrum between 0.6 and 1.0 MeV is from inelastic scattering by plutonium nuclides and elastic scattering by oxygen. The slight buildup between 10 KeV and 100 KeV is from elastic scattering by hydrogen and oxygen. This buildup would increase with added moisture. For this sample the leakage multiplication is about 1.04.

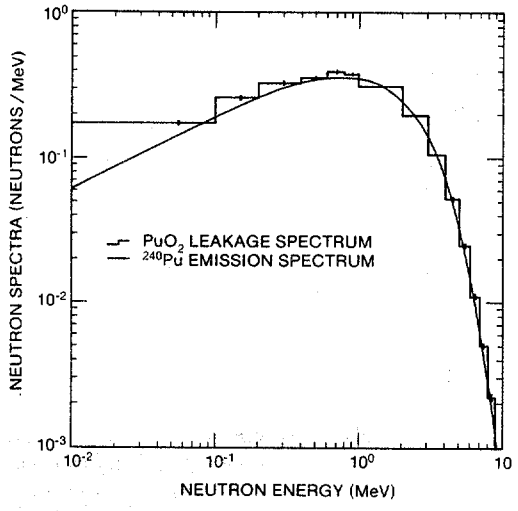

Fig. 14.15 *Neutron leakage spectrum from an 800-g PuO_2 sample (10% ^{240}Pu) assuming an energy spectrum characteristic of ^{240}Pu spontaneous fission. Source neutrons were uniformly distributed in the sample volume.*

14.4 NEUTRON DETECTION EFFICIENCY

Equation 14.1 defines detector efficiency ε as the number of counts produced by the detector per neutron emitted from the sample. This section describes important factors affecting ε for ^{3}He proportional counters moderated by polyethylene. These include arrangement of ^{3}He counters within the polyethylene moderator, moderator design, and the sample leakage spectrum. Also, differences in the energy spectra of signal and background neutrons can be exploited to enhance the signal-to-background counting ratio.

14.4.1 ^{3}He Counter Arrangement

For a fixed moderator geometry, the location and number of ^{3}He proportional counters strongly affects counting efficiency. As an example, a series of efficiency calculations was performed using the MCNP Code (Ref. 7) for a variable number of ^{3}He counters placed within a 1-m-tall annulus of polyethylene. The counting tubes were 1 inch in diameter with 4 atm of ^{3}He (77% thermal-neutron counting efficiency). The internal and external diameters of the annulus were 7 in. (17.8 cm) and 15 in. (38.1 cm), respectively. The ^{3}He counters were evenly spaced within the annulus on a circle 11 in. (27.9 cm) in diameter. A 1-MeV monoenergetic source of neutrons was assumed for the calculations. The two curves in Figure 14.16 show the results of the calculations. The curve belonging to the left ordinate is the absolute counting efficiency versus number of ^{3}He counters. This curve shows a peak counting efficiency of about 29% for 28 ^{3}He counters. Because ^{3}He proportional counters are expensive, absolute counting efficiency is sometimes compromised. The curve belonging to the right ordinate is the counting efficiency per ^{3}He counter (an index of cost effectiveness) versus the number of counters.

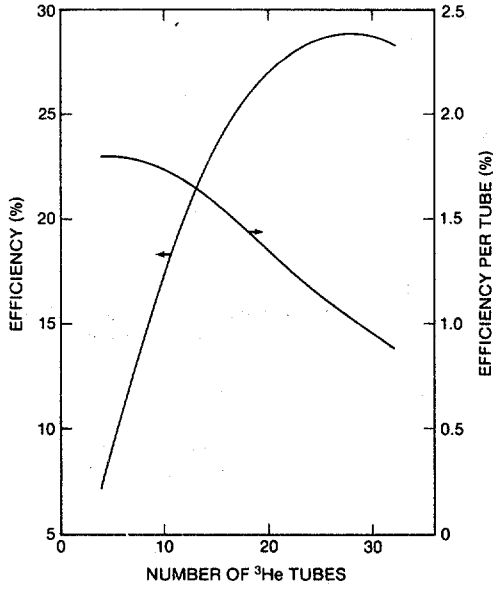

Fig. 14.16 *Results of Monte Carlo calculations of total neutron counting efficiency versus number of ^{3}He counting tubes for the configuration described in Section 14.4.1.*

A reasonable compromise for this example would be 16 ^{3}He counters. Choice of the number of ^{3}He counters would also depend on sample neutron emission intensity and desired counting precision.

14.4.2 Moderator Design

With a fixed number and arrangement of ^{3}He counters, the amount and location of polyethylene moderator can also strongly influence counting efficiency. As an example, calculations were done for a polyethylene slab 10 in. (25.4 cm) long, 6 in. (15.3 cm) tall, and 1.57 in. (4.0 cm) thick (see Figure 14.17). Two ^{3}He counters are embedded within the slab with their axes parallel to the slab's long axis and separated by 2.1 in. (5.3 cm). The counters have a 10-in. active length, 4-atm fill pressure, and 1-in. diam. A ^{252}Cf neutron source is located 15.75 in. (40 cm) from the slab on a line perpendicular to the plane of the ^{3}He counters. The Monte Carlo Code MCNP (Ref. 7) was used to calculate detection efficiency for various polyethylene thicknesses in front of and behind the ^{3}He counters (relative to the source). The Watt fission spectrum was used for the calculations (Equation 14-11) with A = 1.025 and B = 2.926 for ^{252}Cf. These parameters and this slab geometry represent typical values encountered in actual neutron detectors.

Results of the calculations are shown in Table 14-6 and Figure 14.18. The precisions of the calculated relative efficiencies are approximately ±1%. The total slab thickness can be obtained by adding front and back polyethylene thicknesses because thickness is measured from the ^{3}He tube centers. The moderator configuration for highest detection efficiency is 6 cm of polyethylene in front of the ^{3}He counters and 8 cm behind. Note that for fixed rear polyethylene thickness, efficiency peaks and then decreases with increasing

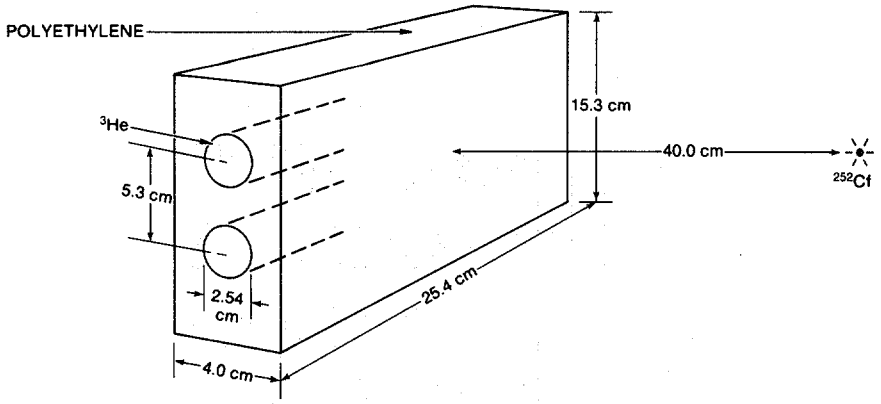

Fig. 14.17 *The geometry used for a series of Monte Carlo calculations of detector efficiency. In the calculations, the thickness of polyethylene in front of and behind the two ^{3}He counters was varied.*

front polyethylene thickness. The decrease is due to neutron capture in hydrogen. For fixed front polyethylene thickness, efficiency approaches an asymptotic value with increasing rear polyethylene thickness. This effect is due to neutron reflection from the rear polyethylene. Often, size and weight constraints limit the total polyethylene moderator thickness to be used. In the U.S., polyethylene is typically purchased in slabs 4 in. (10.2 cm) thick. If, for ease of fabrication, the total slab thickness is constrained to this value, the ^{3}He counters should be placed with 4.6 cm of polyethylene in front and 5.6 cm behind for optimum efficiency.

14.4.3 Effect of Neutron Energy Spectrum

For a particular neutron detector design, the detection efficiency will depend on the incident neutron energy because of the dependence of the ^{3}He(n,p) cross section on neutron energy and the moderating effect of hydrogen in polyethylene. Given a particular neutron leakage spectrum, the detector can be designed to maximize counting efficiency for that spectrum. For applications where the signal-to-background ratio is small, it is desirable to design the detector to discriminate against background neutrons with different energy spectra. Two examples, one for neutrons from UF_6 and one for neutrons from PuO_2, are given in this section.

Collimated neutron slab detectors have been designed to monitor neutron levels in UF_6 gas centrifuge enrichment plants. The detectors are described in Section 15.3.1 and illustrated in Figure 15.4 of Chapter 15. Each detector contains eleven l-in.-diameter ^{3}He counters embedded in a 10.2-cm by 30.5-cm by 61-cm polyethylene slab. The slab is wrapped in cadmium and covered with thick polyethylene shielding except on the 1860-cm^2 open face, which is covered by 1.3 cm of polyethylene. The polyethylene, along with the cadmium, filters out low-energy background neutrons. Figure 14.19 is a schematic cross section of the detector.

Table 14-6. Relative efficiency of a simple slab detector for variable polyethylene moderator in front of and behind the ^{3}He counters

Back Polyethylene Thickness (cm)	Front Polyethylene Thickness (cm)												
	2	2.5	3	3.5	4	4.5	5	5.5	6	6.5	7	7.5	8
2	0.181	0.271	0.334	0.430	0.489	0.521	0.560	0.608	0.622	0.639	0.659	0.615	0.575
2.5	0.242	0.351	0.419	0.508	0.577	0.625	0.661	0.700	0.706	0.717	0.687	0.690	0.644
3	0.301	0.426	0.494	0.596	0.645	0.665	0.713	0.757	0.782	0.765	0.747	0.733	0.692
3.5	0.374	0.497	0.565	0.668	0.717	0.762	0.779	0.821	0.825	0.839	0.807	0.771	0.742
4	0.425	0.547	0.611	0.719	0.769	0.812	0.830	0.872	0.867	0.866	0.826	0.799	0.773
4.5	0.469	0.597	0.650	0.766	0.797	0.847	0.871	0.886	0.908	0.901	0.862	0.839	0.792
5	0.511	0.628	0.688	0.798	0.844	0.887	0.896	0.919	0.946	0.919	0.889	0.849	0.808
5.5	0.547	0.658	0.723	0.833	0.860	0.911	0.917	0.943	0.963	0.944	0.894	0.848	0.810
6	0.564	0.682	0.745	0.843	0.874	0.921	0.941	0.952	0.973	0.965	0.898	0.858	0.815
6.5	0.580	0.696	0.759	0.858	0.895	0.936	0.940	0.962	0.986	0.955	0.910	0.875	0.820
7	0.604	0.703	0.755	0.874	0.909	0.935	0.961	0.975	0.977	0.963	0.921	0.873	0.832
7.5	0.600	0.703	0.773	0.873	0.908	0.945	0.957	0.978	0.989	0.968	0.920	0.873	0.826
8	0.613	0.722	0.775	0.872	0.913	0.954	0.968	0.983	1.000	0.969	0.929	0.883	0.835

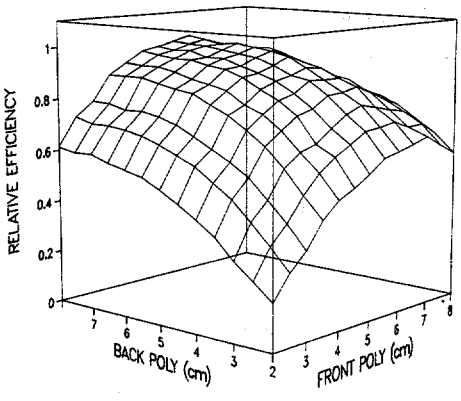

Fig. 14.18 *Relative ^{252}Cf neutron detection efficiency as a function of front and back polyethylene thickness for the small slab detector illustrated in Figure 14.17.*

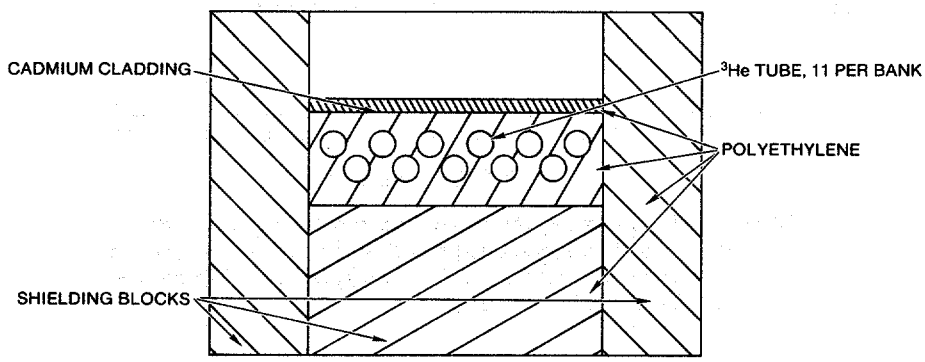

Fig. 14.19 *Cross section of the collimated neutron slab detector.*

The UF_6 monitor was designed to have a neutron energy efficiency profile similar to the $^{19}F(\alpha,n)^{22}Na$ neutron energy spectrum (Figure 14.10). It was also designed to minimize the response to low-energy background neutrons from cosmic rays. This was accomplished by measuring and calculating the effect of three different thicknesses of polyethylene filters on the detector's open face. (Ref. 11). Figure 14.20 is a plot of calculated neutron energy response profiles for three thicknesses of polyethylene: 0, 1.3 cm, and 2.5 cm. The effect of a polyethylene filter is to reduce detection efficiency at all incident neutron energies, but with greater reductions at the lower energies where most of the background neutrons from cosmic rays are found. These calculations indicate that a 1.3-cm filter is a good compromise between high efficiency for 1.0-MeV neutrons and low efficiency for 0.1-MeV neutrons. A more comprehensive study of UF_6 detector optimization for low signal-to-background ratios is reported in Ref. 12.

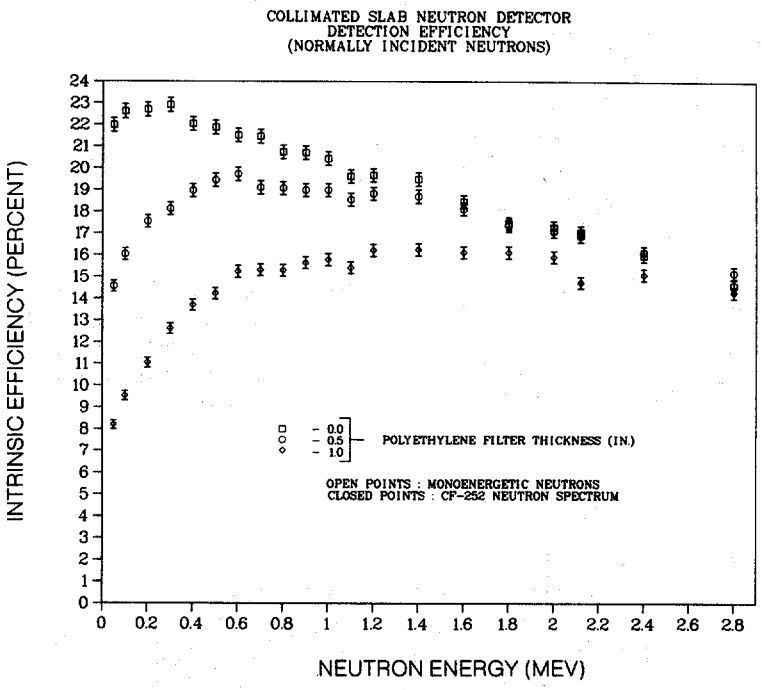

Fig. 14.20 *Calculated detection efficiency of the collimated slab detector as a function of the energy of neutrons normally incident on the open face. Results are shown for three thicknesses of polyethylene filter covering the open face: 0, 1.3, and 2.5 cm.*

The High-Level Neutron Coincidence Counter (HLNCC) is a detector designed primarily for passive neutron coincidence counting of PuO_2 (Ref. 13 and Section 17.2.2 of Chapter 17). Its neutron energy efficiency profile is given in Figure 14.21. If this efficiency profile is compared with the leakage spectrum from a representative PuO_2 sample (Figure 14.15), it can be seen that the HLNCC efficiency is a maximum for neutron energies lower than those actually emitted. In other words, the HLNCC, which was designed to be small and lightweight, contains too little polyethylene and is "undermoderated."

REFERENCES

1. W. B. Wilson, R. T. Perry, and J. E. Stewart, "Neutron Production in UO_2F_2 from the Spontaneous-Fission and Alpha Decay of Uranium Nuclides and Subsequent $^{17,18}O$ (α,n) and ^{19}F (α,n) Reactions," in "Applied Nuclear Data Research and Development, April 1-June 30, 1981," P. G. Young, Comp., Los Alamos National Laboratory report LA-9060-PR (December 1981), p. 50.

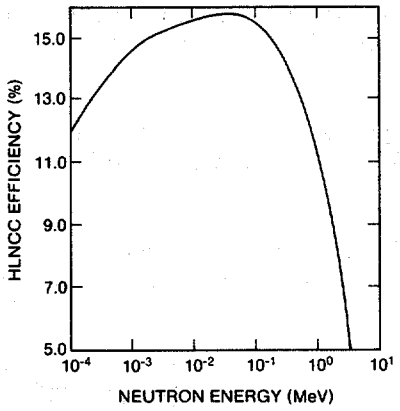

Fig. 14.21 *Calculated detection efficiency of the High-Level Neutron Coincidence Counter (HLNCC) as a function of the energy of neutrons emitted isotropically in the center of the detector well.*

2. R. H. Augustson, R. B. Walton, W. Harbarger, J. Hicks, G. Timmons, D. Shissler, R. Tayloe, S. Jones, R. Harris, and L. Fields, "Measurements of Uranium Holdup in an Operating Gaseous Diffusion Enrichment Plant," in "Proceedings of the ANS/INMM Conference on Safeguards Technology: The Process-Safeguards Interface," Hilton Head Island, South Carolina, November 28-December 2, 1983, US DOE New Brunswick Laboratory, Conf. No. 831106 (August 1984), pp. 77-88.

3. W. B. Wilson, R. T. Perry, J. E. Stewart, T. R. England, D. G. Madlund, and E. D. Arthur, "Development of the SOURCES Code and Data Library for the Calculation of Neutron Sources and Spectra from (α,n) Reactions, Spontaneous Fission, and β^- Delayed Neutrons," in "Applied Nuclear Data Research and Development Semiannual Progress report, October 1, 1982-March 31, 1983," E. D. Arthur, Compiler, Los Alamos National Laboratory report LA-9841-PR (August 1983), p. 65.

4. W. B. Wilson, "Calculations of (α,n) Neutron Production in PuO_2 with Variable Moisture and Fluorine Contamination," Los Alamos National Laboratory memorandum T-2-M-1581, to J. E. Stewart (March 1985).

5. W. B. Wilson, R. T. Perry, and J. E. Stewart, "Neutrons from the Spontaneous Fission of Plutonium Nuclides and from the (α,n) Reactions of Their Decay Alpha Particles with Trace Contaminants of Li, Be, B, C, N, O, F, Na, Mg, Al, Si, Cl, and As in Pu Metal," Los Alamos National Laboratory report (available on request from Group N-1, MS E540).

6. J. E. Stewart, "Neutron Production by Alpha Particles in Thin Uranium Hexafluoride," Los Alamos National Laboratory report LA-9838-MS (July 1983).

7. Los Alamos Monte Carlo Group X-6, "MCNP - A General Monte Carlo Code for Neutron and Photon Transport, Version 2B," Los Alamos Scientific Laboratory report LA-7396-M, Rev. (November 1979).

8. N. Ensslin, J. Stewart, and J. Sapir, "Self-Multiplication Correction Factors for Neutron Coincidence Counting," *Nuclear Materials Management* VIII (2), 60 (1979).

9. E. D. Cashwell, J. R. Neergaard, W. M. Taylor, and G. D. Turner, "MCN: A Neutron Monte Carlo Code," Los Alamos Scientific Laboratory report LA-4751 (1972).

10. R. B. Walton, T. D. Reilly, J. L. Parker, J. H. Menzel, E. D. Marshall, and L. W. Fields, "Measurements of UF_6 Cylinders with Portable Instruments," *Nuclear Technology 21,* 133 (1974).

11. J. E. Stewart and S. M. Simmonds, "Neutron Energy Response of an Area Neutron Monitor," in "Safeguards and Security Progress Report, January-December 1984," Los Alamos National Laboratory report LA-10529-PR (1986), p. 85.

12. J. E. Stewart and H. O. Menlove, "Design Study of an Optimized In-Cascade Neutron Monitor for Centrifuge Plants," in "Safeguards and Security Status Report: February-July 1982," Los Alamos National Laboratory report LA-9595-PR (February 1983), pp. 57-63.

13. M. S. Krick and H. O. Menlove, "The High-Level Neutron Coincidence Counter (HLNCC): User's Manual," Los Alamos Scientific Laboratory report LA-7779-M (ISPO-53) (June 1979).